UCLA
UCLA Previously Published Works

Title
Engineering a highly elastic bioadhesive for sealing soft and dynamic tissues

Permalink
https://escholarship.org/uc/item/7xh27027

Journal
Journal of Biomedical Materials Research Part B Applied Biomaterials, 110(7)

ISSN
1552-4973

Authors
Ghovvati, Mahsa
Baghdasarian, Sevana
Baidya, Avijit
et al.

Publication Date
2022-07-01

DOI
10.1002/jbm.b.35012

Peer reviewed

eScholarship.org Powered by the California Digital Library
University of California

Author Manuscript

Author Manuscript

Author Manuscript

Author Manuscript

HHS Public Access

Author manuscript

J Biomed Mater Res B Appl Biomater. Author manuscript; available in PMC 2023 July 01.

Published in final edited form as:

J Biomed Mater Res B Appl Biomater. 2022 July ; 110(7): 1511–1522. doi:10.1002/jbm.b.35012.

Engineering a highly elastic bioadhesive for sealing soft and dynamic tissues

Mahsa Ghovvati[1], **Sevana Baghdasarian**[1], **Avijit Baidya**[1], **Jharana Dhal**[1], **Nasim Annabi**[1,*]

[1]Department of Chemical and Biomolecular Engineering, University of California - Los Angeles, Los Angeles, CA 90095, USA.

Abstract

Injured tissues often require immediate closure to restore the normal functionality of the organ. In most cases, injuries are associated with trauma or various physical surgeries where different adhesive hydrogel materials are applied to close the wounds. However, these materials are typically toxic, have low elasticity, and lack strong adhesion especially to the wet tissues. In this study, a highly stretchable composite hydrogel consisting of gelatin methacrylol catechol (GelMAC) with ferric ions, and poly (ethylene glycol) diacrylate (PEGDA) was developed. The engineered material could adhere to the wet tissue surfaces through the chemical conjugation of catechol and methacrylate groups to the gelatin backbone. Moreover, the incorporation of PEGDA enhanced the elasticity of the bioadhesives. Our results showed that the physical properties and adhesion of the hydrogels could be tuned by changing the ratio of GelMAC/PEGDA. In addition, the *in vitro* toxicity tests confirmed the biocompatibility of the engineered bioadhesives. Finally, using an *ex vivo* lung incision model, we showed the potential application of the developed bioadhesives for sealing elastic tissues.

1 | INTRODUCTION

In recent years, there has been a significant demand in developing ideal bioadhesives to replace traditional methods for wound closure during and post-surgery[1–10]. The traditional methods utilized for wound closure, such as sutures and staples, are time-consuming and typically result in more trauma and a higher risk of infection. Furthermore, sealing of soft tissues such as artery walls, nerves, and those which are not easily accessible during surgery, require the application of adhesives to achieve better closure[8,10–17]. It is also critical that the tissue is held together during the wound healing process, especially when undergoing mechanical stresses. Therefore, an ideal tissue adhesive should be able to effectively close and heal the wound. For soft and dynamic tissues such as lung and heart, adhesives need to withstand the high physiological pressure and therefore need to possess high stretchability to preserve the function of the native tissues[3]. In addition to comparable mechanical properties to native tissue, an ideal adhesive sealant should exhibit a tunable degradation characteristic and high biocompatibility[18–20].

*Corresponding author. nannabi@ucla.edu.

CONFLICT OF INTEREST

The authors declare that there is no conflict of interest.

Author Manuscript Author Manuscript Author Manuscript Author Manuscript

For the repair of dynamic tissues such as lung and heart, bioadhesives with high elasticity and stretchability are considered to be suitable candidates[21–23]. As it has been reported, the elasticity of the biomaterials influences critical cellular functions[24,25]. It is challenging to design and engineer hydrogels with similar elasticity as the native tissue to withstand high mechanical loads in physiological environments[13,26–29]. To address this limitation, numerous elastin-like macromolecules have been used to develop various bioadhesives for wound repair application. For instance, a human protein-based stretchable hydrogel named methacryloyl-substituted tropoelastin (MeTro) was developed to seal elastic tissues such as lungs and arteries[26]. Also, MeTro was combined with nanostructured graphene oxide to further enhance its elasticity and toughness[30]. In another study, Han *et al.* have designed polydopamine- and polyacrylamide-based hydrogels with high stretchability, mechanical properties, and adhesion to wet tissue[31]. Furthermore, Sun, J. *et al.* reported synthesis of hydrogels which were stretched up to 20 times their original length fracture energies of ~9,000 J m^{-2} [32]. Also, in one study, a sealant consisted of an adhesive surface and a dissipative matrix was developed, which was tested on a beating porcine heart *in vivo*. The results of their study showed no leakage under strains up to 100% during cardiac expansion and complete sealing after tens of thousands of beating cycles[4]. In addition, there have been several developments in the design of tough and stretchable hydrogels for wet surface application[32–37]. Although these engineered materials have shown strong adhesion and high elasticity, biodegradability and biocompatibility remain as two limiting factors in their successful clinical application and translation. For example, synthesis of some hydrogels/adhesives involves toxic chemicals such as graphene oxide[37], organic solvents[33], or toxic monomers such as acrylamide[32,35]. In addition, the fabrication of some of these adhesives needs prolonged exposure to UV light[14] hindering their clinical translation. Therefore, there is an existing gap in the design and development of stretchable sealants with high biocompatibility for clinical use.

In this work, we aim to address the existing limitations by developing a biodegradable, biocompatible, stretchable, and adhesive hydrogel for soft tissue sealing and repair. We engineered composite bioadhesive based on gelatin methacrylol catechol (GelMAC) and poly (ethylene glycol) diacrylate (PEGDA), which were formed through two steps crosslinking using ferric ions and visible light. The synthesis of GelMAC was biologically inspired by marine mussels. The strong underwater adhesion of mussels to surfaces is mediated by the mussel adhesive proteins which are abundant in a catecholic amino acid, 3,4-dihydroxyphenylalanine (Dopa)[38]. This robust adhesion is driven by the mechanism of forming hydrogen bonding, metal chelation, π-π interactions, or π-cation interactions with the tissue surface[39–43]. We hypothesized that catechol moieties of GelMAC will enhance the adhesion to the tissue while ferric ions will assist in further crosslinking by chelation[44]. Also, the addition of PEGDA will provide high stretchability, which is critical for the application of bioadhesive in sealing elastic tissues. We characterized the physical properties of the bioadhesive formed by using different ratios of GelMAC/PEGDA. We also assessed the *in vitro* biocompatibility of the engineered bioadhesives using NIH 3T3 fibroblast cells. To evaluate the capability of the hydrogel for sealing elastic tissues, we tested the burst pressure of the optimized bioadhesive formulation in an *ex vivo* lung incision model.

Author Manuscript Author Manuscript Author Manuscript Author Manuscript

2 | MATERIALS AND METHODS

2.1 | Materials

Gelatin from porcine skin, poly (ethylene glycol) (PEG), methacrylic anhydride, acryloyl chloride, (Benzotriazol-1-yloxy)tris(dimethylamino)phosphonium hexafluorophosphate (BOP), 1-Hydroxybenzotriazole hydrate (HOBt), dopamine hydrochloride, Eosin Y disodium salt, Triethanolamine (TEA), N-Vinylcaprolactam (VC), 3-(Trimethoxysilyl)propyl methacrylate (TMSPMA), and hydroquinone were all purchased from Sigma-Aldrich. Dulbecco's phosphate-buffered saline (DPBS) was obtained from HyClone. Collagenase type II was purchased from Worthington Biochemical Co. PrestoBlue cell viability reagent, and live/dead viability kits were purchased from Invitrogen. Dulbecco's Modified Eagle Medium (DMEM), Nu-serum, and Penicillin-Streptomycin (Pen-Strep) were obtained from Gibco).

2.2 | Synthesis and characterization of GelMAC/PEGDA hydrogels

Synthesis of GelMAC: To synthesis GelMAC prepolymer, gelatin (4 mg/ml) was dissolved in water at 50°C. Next, 2 mM BOP, 2 mM HOBt, 20 mM dopamine hydrochloride, and 20 mM of triethylamine were added and kept for 12 h under N_2 atmosphere. Dopamine conjugated gelatin was finally precipitated with cold acetone and further reacted with methacrylic anhydride as previously described[45]. Briefly, dopamine-modified gelatin was dissolved in DPBS at a concentration of 10% (w/v) and heated to 50°C. Next, 8% (v/v) methacrylic anhydride was added dropwise to the solution under continuous stirring at 50°C and allowed to react for 3 h. Finally, the reaction was stopped by diluting the reaction mixture with DPBS. The resulting solution was dialyzed against deionized water at 40–50°C for 5 days, followed by the 4 days lyophilization.

PEGDA synthesis: PEDGA was synthesized through the chemical conjugation of PEG molecules with acryloyl chloride in toluene. Briefly, 30 g of PEG (20 kDa) was dissolved in toluene and mixed with 2.5 ml trimethylamine. Next, a solution containing 1 ml acryloyl chloride and 10 ml dried toluene was added to the reaction mixture and kept for 2 h. Finally, the reaction mixture was filtered through a silica bed and collected in a flask containing 200μl of 30–50 ppm hydroquinone solution in acetone. The chemically modified PEG was precipitated in hexane and stored at −80°C for future use.

Preparation of GelMAC/PEGDA hydrogels: GelMAC/PEGDA prepolymer solutions were prepared by mixing 100/0, 75/25, 50/50, 25/75, and 0/100 ratios of GelMAC/PEGDA polymers in a photocrosslinker solution (in water) while maintaining total polymer concentration at 20% (w/v). The photocrosslinker solution was prepared by dissolving photocrosslinking reagents (0.1 mM Eosin Y, 1% (w/v) VC, and 1.5 % (w/v) TEA), and 2.5 mM ferric ions (Fe^{3+}) in water at room temperature. Hereafter, the final prepolymer solutions were continuously stirred at 50 °C for 2–3 h followed by the application over the tissue surface or other characterization tests. Finally, to form the GelMAC/PEGDA bioadhesives, the mixture was exposed to a visible light (*450–550 nm*) for 4 min.

Author Manuscript Author Manuscript Author Manuscript Author Manuscript

2.3 | *In vitro* adhesive properties of GelMAC/PEGDA hydrogels

To assess the adhesive properties of the developed hydrogels, wound closure (ASTM F2458-05) and burst pressure (ASTM F2392-04) tests were performed. For the wound closure test, two rectangular porcine lung tissues were cut (1 cm × 2 cm) and fixed onto two glass slides (2 cm × 6 cm) with superglue. Next, the tissues were brought together (at their 1cm width side), and 50 μl of the GelMAC/PEGDA prepolymer solution was injected at their interface, covering a total surface area of 1 cm^2. Finally, the injected prepolymer solution was photocrosslinked using visible light for 4 min. The adhesive strengths of the hydrogels were calculated at the failure point while being pulled at a strain rate of 1 mm/min using a mechanical tester (Instron 5943) with a 100 N load cell.

To perform the burst pressure test, a small hole (2 mm in diameter) was created at the center of a collagen sheet seal (40 cm × 40 cm). A 40 μl of GelMAC/PEGDA prepolymer solution was then injected at the defect site and immediately photocrosslinked using visible light for four min. One ml of DPBS was then injected over the photocrosslinked hydrogel layer. Next, air was pumped at a constant rate of 10 mL/min using a syringe pump (New Era Pumps Systems Inc., NE-1000). The internal pressure was continuously measured and recorded (with a PASCO wireless pressure sensor and software) until the seal burst and first air bubbles were observed.

2.4 | Tensile properties of the GelMAC/PEGDA hydrogels

A tensile test was performed using an Instron 5943 mechanical tester with a 100 N load cell. GelMAC/PEGDA hydrogels were prepared using rectangular polydimethylsiloxane (PDMS) molds (dimensions 12 mm × 6 mm × 1 mm). The hydrogels were placed between two pieces of double-sided tape within tension grips and extended at a constant strain rate of 1 mm/min until failure. Elastic moduli of the GelMAC/PEGDA hydrogels were calculated from the slope of the linear region of the resulting stress-strain curves[46]. The tensile strain (extensibility) and ultimate stress values were obtained at the failure points (the tensile strain (mm) and load (N) were measured using the Bluehill Universal software).

2.5 | *In vitro* swelling and mass changes of the GelMAC/PEGDA hydrogels

The swellability of the hydrogels was assessed by calculating the amount of DPBS uptake at 37°C over time. GelMAC/PEGDA hydrogels were prepared using cylindrical PDMS mold (diameter: 5 mm, height: 3 mm). The initial weight of the GelMAC/PEGDA hydrogels immediately after crosslinking was measured and recorded (W_1). Hydrogel samples were then placed in 24 well plates and incubated in DPBS at 37°C. At each time point (1, 3, 6, 24, and 48 h), samples were removed from the DPBS solution and weighed (W_2). The swelling ratio (%) was calculated using Equation 1:

$$\text{Swelling ratio}(\%) = \frac{W2 - W1}{W1} \times 100 \quad \text{Equation 1}$$

To evaluate the mass change of the GelMAC/PEGDA hydrogels in a simulated body fluid, cylindrical hydrogel samples (diameter: 5 mm, height: 3 mm) were prepared and weighed (W_1) immediately after photocrosslinking. The samples were placed in a 24 well plate

Author Manuscript Author Manuscript Author Manuscript Author Manuscript

containing 5 U/mL of collagenase type II in DPBS solution at 37°C for up to 4 days. Fresh collagenase solution was replaced every other day. At each time point (1, 2, 3, 4 days), the samples were removed from the solution and weighed (W_2) to determine the mass changes after degradation. The normalized mass (%) was calculated using Equation 2:

$$\text{Normalized mass}(\%) = \frac{W2}{W1} \times 100 \quad \text{Equation 2}$$

2.6 | *In vitro* biocompatibility of GelMAC/PEGDA hydrogels

To assess several the *in vitro* biocompatibility of the hydrogels, NIH 3T3 fibroblast cells were cultured on the surfaces of the hydrogels. Cellular spreading and viability analysis was performed using the fluorescence-based live/dead stain kit. In addition, the metabolic activity of the cells was assessed using a PrestoBlue cell viability reagent.

To form the hydrogels, a 12 μl drop of hydrogels precursor was injected at a spacer with 120 μm height. A TMSPMA-coated glass slide was placed on top of the hydrogel precursor and immediately photocrosslinked using visible light for 20 sec. This step was followed by seeding the surface of the hydrogels with 3T3 cells at a density of 2×10^4 cells per scaffold and placed in 24-well plates containing 1 ml growth medium, DMEM, supplemented with 10% (v/v) Nu-serum and 1% (v/v) Pen-Strep. Samples were incubated at 37°C (in a 5% CO_2 humidified atmosphere) for one week, and the growth medium was replaced every 48 h.

The viability and spreading of 3T3 cells grown on the surfaces of the hydrogels were assessed utilizing a live/dead stain kit according to the manufacturer's instructions. Briefly, samples were stained with fluorescent dyes, 0.5 μl/ml of calcein-AM (green-fluorescent), and 2 μl/ml of ethidium homodimer-1 (EthD-1) (red-fluorescent), in DPBS for 30 min at 37°C. The cells possessing green fluorescence were deemed as live, and the ones appearing with red fluorescence were assigned as dead. Fluorescent images were taken at days 1, 4, and 7 post-seeding utilizing a Zeiss Axio Observer Z1 inverted microscope and were evaluated using the ImageJ software. In addition, cell viability was defined as the number of live cells divided by the total number of cells (both live and dead cells).

Moreover, the metabolic activity of cells was evaluated at days 1, 4, and 7 post-seeding using PrestoBlue cell viability reagent according to the manufacturer's instructions. Briefly, samples were incubated in 400 μl of DMEM with 10% PrestoBlue for 40 min at 37°C. The resulting fluorescence was assessed using a Synergy HT plate reader (BioTek) (fluorescence excitation/emission: 535/590 nm). All the aforementioned experiments were repeated with quadruplicate samples ($n \geq 4$) to ensure statistical significance.

2.7 | *Ex vivo* burst pressure test using porcine lung

The burst pressures of the GelMAC/PEGDA hydrogels, and the clinically available CoSeal surgical sealant (*Baxter Healthcare Corporation*) ($n = 3$) were determined utilizing an *ex vivo* porcine lung incision model as previously described[26]. Fresh lungs were obtained, kept at 4° C, and were tested against any defects prior to experimentation. A 20 L pan was used as a reservoir and filled with water at 37°C. Each lung was connected to a

Author Manuscript Author Manuscript Author Manuscript Author Manuscript

time-cycled anesthesia ventilator (*Honeywell 2002^{PRO}, 300–1600mL*) and was inflated at a constant positive pressure of 0.01 kPa for 10 min to ensure there were no pre-existing defects. Lobes exhibiting air leaks or failing to appropriately inflate were excluded from the test. A standardized superficial wound, 1cm in diameter, was created on the left lobe of the deflated porcine lung. The wound was created by first placing a cylindrical mold on the visceral pleural of the lung. Next, ethyl 2-cyanoacrylate-based glue (*Scotch® Super Glue*) was injected on the entire surface area enclosed by the mold and was left to dry for 4 min. The visceral pleural layer was then removed utilizing a microtome blade, creating a superficial uniform defect. Finally, the hydrogel solution was injected at the wound site and photopolymerized for 4 min with visible light. The burst pressure of the hydrogel was determined by constantly increasing the ventilation pressure and recorded at the appearance of the first air bubbles rising from the burst seal.

3 | RESULTS

3.1 | Synthesis and characterization of GelMAC/PEGDA hydrogels

In this work, an adhesive and stretchable hydrogel was engineered based on gelatin and PEG backbones for soft tissue sealing and repair. The molecular structures of chemically modified GelMAC and PEDGA along with the synthesis of the GelMAC/PEGDA hydrogels incorporating ferric ions are schematically presented in Figure 1a. Functional interactions between GelMAC and PEGDA comprised of covalent bonding upon photocrosslinking and ferric ion induced non-covalent chelation interactions. In the first step, to incorporate high sealing ability, catechol moieties with significant contribution towards the mussel adhesion were covalently conjugated by using dopamine molecules (dopamine molecules possess catechol moieties which is dihydroxybenzene and an amine functional group). In this case, amine groups of dopamine molecules formed amide linkage with carboxylic groups from gelatin biopolymer. Next, as-synthesized, dopamine-modified gelatin was further functionalized with methacrylic groups sequentially through the nucleophilic substitution reaction between the amine groups and methacrylic anhydride to form GelMAC. Similarly, PEG molecules were separately modified with acryloyl chloride to synthesize PEGDA. Here, Eosin Y, TEA/VC were used to initiate the photocrosslinking process to covalently bond the acrylic groups of both GelMAC and PEGDA polymers. In addition, ferric ions were added to the prepolymer solution to improve the gelation through the interaction among the catechol moieties of dopamine. Application of the prepolymer solution over the ruptured lung tissue surface followed by visible light photocrosslinking to form an adhesive is schematically presented in Figure 1a. The proton nuclear magnetic resonance (^{1}H NMR) spectra of GelMAC and PEGDA polymers (Figure 2b,c) confirmed the chemical conjugation of methacrylate groups with gelatin and PEG backbones, respectively. The peaks at ~5.3 and 5.6 (Figure 1b), and ~5.9 and 6.3 (Figure 1c) corresponded to the vinyl C-H proton of GelMAC and PEGDA, respectively. Since there are several amine and OH groups on the gelatin backbone, the degree of methacrylation for GelMAC could be calculated by integrating the gelatin and GelMAC ^{1}H NMR spectra. The degree of methacrylation for GelMAC was found to be ~40–45%. On the other hand, PEG molecules having terminal OH groups were methacrylated only on their terminal ends with a degree of methacrylation ~70%. Figure 1d shows the uncrosslinked and photocrosslinked ^{1}H NMR

Author Manuscript Author Manuscript Author Manuscript Author Manuscript

spectra of prepolymer and crosslinked GelMAC/PEGDA hydrogel (50/50 ratio). Integrated ^{1}H NMR spectra showed the degree of crosslinking ~77%. The notable decrease in the vinyl C-H proton peak (at 5.3 and 5.6) in the crosslinked hydrogel spectrum confirmed the photocrosslinking through the incorporated methacrylate functionality.

3.2 | *In vitro* adhesive properties of GelMAC/PEGDA hydrogels

We assessed the adhesive properties of GelMAC/PEGDA hydrogels to the wet tissue surface using porcine lung tissue and collagen sheet. The ratios of GelMAC/PEGDA prepolymers were varied between 0–100 while total polymer concentration was kept at 20% (w/v). The schematic shown in Figure 2a illustrates various chemical interactions between the GelMAC/PEGDA hydrogel and the hydrophilic tissue surface. Here, along with various hetero atoms (O, N) induced hydrogen bonding interactions, during the photocuring process, several covalent bonding interactions are also feasible. These include interaction between methacrylate groups of hydrogel and amine and thiol groups of the tissue surface. For non-covalent interactions, tissue surfaces enriched with hydrophilic hydroxyl, carboxyl, and amine groups form hydrogen bondings with the applied hydrogel having amine, carboxyl, hydroxy, and catechol (from dopamine) groups. Figure 2b demonstrates a schematic of the wound closure test used to measure the adhesion of the bioadhesive to porcine lung tissue. Our results showed that the adhesive strength of GelMAC/PEGDA hydrogels decreased with increasing PEGDA polymer concentration (Figure 2c). For example, 100/0, 50/50, and 0/100 ratios of GelMAC/PEGDA hydrogels (containing no ferric ions) exhibited adhesive strength of 37.96 ± 2.54 kPa, 23.76 ± 2.20 kPa, and 15.10 ± 1.89 kPa, respectively. The adhesion strengths of all the engineered formulations were higher than the dopamine-integrated gelatin methacryloyl (DA@GelMA) and polydopamine-integrated gelatin methacryloyl (PDA@GelMA) patches, reported by Montazerian *et al.*[47]. In addition, the engineered hydrogel also showed improved adhesive performance as compared to the catechol containing hydrogels prepared with four-armed poly(ethylene glycol) (PEG-D4).[48], and poly(ethylene glycol)-co-poly(glycerol sebacate) (QCSP/PEGS-FA)[9]. Further studies with the GelMAC/PEGDA hydrogels also showed no significant change in the adhesive strength with and without ferric ions.

We also performed a burst pressure test to measure the maximum pressure the engineered bioadhesives are able to withstand before failure, an important parameter for designing biomaterials to be used as a sealant for wound healing applications. The schematic of the burst pressure measurement setup is shown in Figure 2d. Similar to the wound closure test, the burst pressure or the hydrogels decreased with increasing PEGDA concentration, but the hydrogels containing ferric ions showed higher burst pressure on the collagen sheet compared to hydrogels formed without ferric ions (Figure 2e). Improved burst pressure values for the hydrogels containing ferric ions could be due to the increased non-covalent crosslinking interactions between ferric ions and dopamine through chelation mechanism, presented in figures 1a & 2e. For example, the burst pressure value for 50/50 ratio of GelMAC/PEGDA hydrogels incorporating ferric ions was found to be 20 ± 3 kPa which was significantly higher than the corresponding value for the same ratio of hydrogels containing no ferric ions (12.5 ± 1 kPa).

Author Manuscript Author Manuscript Author Manuscript Author Manuscript

3.3 | Tensile properties of the GelMAC/PEGDA hydrogels

To evaluate the tensile properties of the fabricated hydrogels, the ratios of GelMAC/PEGDA biopolymers were varied from 100/0 to 0/100 while keeping the total polymer concentration at 20% (w/v). A schematic and a representative image of the tensile test are illustrated in Figure 3a. The extensibility (strain to failure) of the fabricated hydrogels is shown in Figure 3b. It was found that increasing the PEGDA ratio up to 100 enhanced the extensibility of the composite hydrogels. However, further increases in PEGDA concentration decreased the extensibility. For example, 75/25, 50/50, and 25/75 ratios of GelMAC/PEGDA hydrogels, containing ferric ions exhibited 44.56 ± 4.12 %, 98.30 ± 4.33 %, and 72 ± 5.71 % extensibility, respectively. Improved extensibility of 50/50 GelMAC/PEGDA hydrogels in the rage of 98.30 ± 4.33 % was approximately 1.5 and 1.2-fold higher as compared to the previously reported nano hydroxyapatite (nHA) based composite hydrogels[49], and MeTro/GelMA hydrogels, respectively[50]. Meanwhile, similar range of extensibility was observed for an adhesive hydrogel prepared with inorganic carbon nanotubes material and used for wound healing application[8]. Whereas, GelMAC/PEGDA hydrogels were solely designed with organic macromolecules which could help in maintaining the biodegradability and biocompatibility of the engineered material.

Moreover, as shown in Figure 3c, the elastic moduli of the GelMAC/PEGDA hydrogels decreased as the PEGDA prepolymer concentration was increased. For instance, the hydrogels fabricated with 75/25, 50/50, and 25/75 ratios of GelMAC/PEGDA polymers (all without ferric ions) demonstrated elastic modulus values of 146.43 ± 6.30, 65.11 ± 10.59 kPa, and 61.53 ± 2.51 kPa, respectively.

Similar to the elastic modulus behavior, the ultimate stress of the GelMAC/PEGDA hydrogels was observed to decrease with increasing PEGDA concentration (Figure 3d). For example, ultimate stress values corresponding to 100/0, 50/50, and 0/100 ratios of GelMAC/PEGDA hydrogels (all without ferric ions) were 87.02 ± 7.59 kPa, 67.12 ± 2.36 kPa, and 27.90 ± 4.11 kPa. This could be easily explained with the contribution of ferric ions in the GelMAC/PEGDA hydrogels. Chemically, ferric ions can interact with the catechol groups through non-covalent chelation mechanism and increase the crosslinking density[51]. Therefore, the hydrogels with catechol moieties can easily form a secondary network with ferric ions and contribute towards the improvement of mechanical charecterestics[52–55]. Similarly, in this case also, 100/0 GelMAC/PEDGA hydrogel showed higher ultimate strength values due to the ferric ion induced increased non-covalent crosslinking density as compared to the GelMAC/PEDGA hydrogels with reduced GelMAC concentrations, and lack of interactions between ferric ions and PEGDA.

3.4 | *In vitro* swelling and mass changes of the GelMAC/PEGDA hydrogels

The swelling of the bioadhesives formed at varying ratios of GelMAC/PEGDA polymers with and without ferric ions showed a rapid water uptake up to the 6 h incubation at 37°C but exhibited no significant change afterward, demonstrating that equilibrium states were reached at this time point (Figure 4 a,b). In addition, the hydrogels synthesized with higher concentrations of PEGDA exhibited higher water uptake ability. Furthermore, the results demonstrated that only pure GelMAC degraded during the 4 days incubation at 37°C in

Author Manuscript Author Manuscript Author Manuscript Author Manuscript

collagenase solution, and the hydrogels containing PEGDA just swelled (Figure 4 c,d). There were also no significant differences in swelling ratios and degradation rates of the GelMAC/PEGDA hydrogels with and without ferric ions.

3.5 | *In vitro* biocompatibility of GelMAC/PEGDA hydrogels

Herein, we evaluated cytocompatibility of the two optimized experimental groups: 100/0, and 50/50 ratios of GelMAC/PEGDA hydrogels (at 20% (w/v) total polymer concentration) incorporating ferric ions named GelMAC-Fe and (GelMAC/PEGDA)-Fe, respectively. Due to desirable mechanical properties of (GelMAC/PEGDA)-Fe, this formulation was selected for cell study and *ex vivo* burst pressure test and was compared to the GelMAC-Fe hydrogel as control.

Figure 5a represents the live/dead images of 3T3 cells seeded on the surfaces of the hydrogels. The cell proliferation and the quantitative cell viability at days 1, 4, and 7 post-seeding are shown in Figure 5b and Figure 5c, respectively. As shown in Figure 5b, the number of cells increased consistently until day 7 post-seeding for both GelMAC-Fe and (GelMAC/PEGDA)-Fe hydrogels. Furthermore, the cell viability in (GelMAC/PEGDA)-Fe hydrogels and controls remained >95% (Figure 5c).

The metabolic activity of 3T3 cells was also measured on 1, 4, and 7 days post-seeding (Figure 5d). As higher fluorescence intensity values correlate to greater total metabolic activity, it was found that the metabolic activity increased consistently until day 7 post-seeding. For example, (GelMAC/PEGDA)-Fe hydrogels exhibited fluorescence intensity of 1896.5 ± 196.5 a.u., 3050 ± 50 a.u., and 4395 ± 235 a.u. on 1, 4, and 7 days post-seeding.

3.6 | *Ex Vivo* burst pressure test using porcine lung

As mentioned before, due to the observed adhesive and highly elastic characteristics of the optimized (GelMAC/PEGDA)-Fe hydrogel formulation, we proceeded to test its burst pressure ability in an *ex vivo* porcine lung incision model. A 1cm-wide circular defect was created as described previously (Figure 6a(i)). The removed visceral pleural layer is illustrated in Figure 6a(ii). The optimized (GelMAC/PEGDA)-Fe prepolymer solution was applied at the defect site on porcine lungs to seal the wound and was photopolymerized immediately following its application (Figure 6a(iii)). A picture of the wound site after sealing is shown in Figure 6a(iv). A representative graph depicting the stepwise pressure increase over time during testing is shown in Figure 6b. The average burst pressure values were found to be 1.83 ± 0.14 kPa, 1.93 ± 0.31 kPa, and 2.50 ± 0.32 kPa for GelMAC-Fe, (GelMAC/PEGDA)-Fe, and CoSeal, respectively (Figure 6c). According to these results, (GelMAC/PEGDA)-Fe exhibited a similar sealing ability to the GelMAC-Fe hydrogel. Therefore, we were able to achieve a comparable burst pressure ability by incorporating highly adhesive GelMAC hydrogel without compromising the sealing ability of the developed composite hydrogel. Moreover, the obtained results confirm that the engineered (GelMAC/PEGDA)-Fe hydrogel has a comparable burst pressure value to the CoSeal surgical sealant.

Author Manuscript Author Manuscript Author Manuscript Author Manuscript

4 | DISCUSSION

Despite the existence of diverse surgical sealants, they have several inherent limitations, such as mechanical mismatch with tissues, low adhesion, and low biocompatibility. Therefore, none of the existing surgical sealants/adhesives create proper sealing[14,56]. Here, to address these limitations, we propose an alternative tissue adhesive made from GelMAC, PEGDA, and ferric ions.

The interaction between the engineered hydrogels and wet tissue surface resulted in strong adhesion within 4 min exposure to visible light. Mechanistically, tissue surfaces enriched with amine (NH_2), hydroxyl (OH), thiol (SH), and carboxylic (COOH) groups can form different covalent and non-covalent interactions with the hydrogel material. While covalent bonding interactions are facilitated through the Michael addition reaction, non-covalent interactions are mostly governed by the hydrogen bonding interaction.

Herein, PEGDA molecules with enriched oxygen atoms readily contribute towards the formation of intermolecular hydrogen bonding interactions between GelMAC (acceptor: amine, hydroxyl, carboxyl group) and PEGDA (doner) macromolecules. These impart the stretchable characteristic of the composite hydrogel material. However, a higher concentration of PEGDA results in a reduction of the stretchability of the hydrogels due to the lack of donor sites (functional groups from GelMAC).

Also, upon increasing PEGDA concentration, ultimate stress values of the resulting hydrogels (which was related to the cohesive interaction between the polymeric chains) were observed to decrease. This can be explained considering the decrease in the concentration of methacrylate groups which form the covalent linkages upon photocrosslinking (each PEGDA macromolecule can be methacrylated terminally whereas gelatin is enriched with amine/OH groups on its backbone and can possess multiple methacrylate groups).

Moreover, higher burst pressure values obtained for the hydrogels containing ferric ions highlight the contribution of ferric ions through the catechol-tissue interactions in enhancing the cohesion strength of the hydrogels.

In addition, the hydrogels containing higher PEGDA concentrations exhibited higher water uptake ability owing to the presence of a large number of oxygen atoms in the poly(ether) backbone of the PEGDA macromolecule. These oxygen atoms are capable of binding to the hydroxyl groups of water and therefore increasing the swellability. Also, the hydrogels containing higher PEGDA concentration (with and without ferric ions) were found to have slower degradation rates in the enzymatic solution due to the presence of the hydrophilic interactions between PEGDA macromolecules and water molecules.

The *in vitro* cytotoxicity assessment of the (GelMAC/PEGDA)-Fe hydrogels also confirms their excellent biocompatibility. Furthermore, the *ex vivo* data confirm that these highly elastic hydrogels are capable of sealing pulmonary air leakages in an *ex vivo* porcine lung incision model. However, further experiments are needed to evaluate the efficacy of the developed sealant *in vivo* in a porcine model of severe lung injury. Taken together, the

Author Manuscript Author Manuscript Author Manuscript Author Manuscript

results show that the developed hydrogels can be regarded as an excellent candidate for biomedical applications.

5 | CONCLUSIONS

In this work, a photocrosslinkable composite sealant comprised of highly adhesive GelMAC and highly extensible PEGDA polymers was developed. The inclusion of these two biopolymers with distinct physiochemical properties, along with ferric ions, resulted in a highly tunable and elastic hydrogel system. We have characterized and optimized the physical, mechanical, and adhesive properties of the engineered hydrogels and have found that (GelMAC/PEGDA)-Fe hydrogel system yielded the most optimum properties as a soft tissue sealant. In addition, the *in vitro* 2D cell studies utilizing NIH 3T3 fibroblast cells confirmed the high biocompatibility of the engineered hydrogels. Moreover, the (GelMAC/PEGDA)-Fe sealant was found to be capable of sealing lung injuries in an *ex vivo* porcine lung incision model with comparable sealing ability to CoSeal, a widely available commercial sealant. Overall, our results demonstrate the remarkable potential of the engineered (GelMAC/PEGDA)-Fe hydrogels as a highly elastic soft tissue sealant.

ACKNOWLEDGEMENTS

N.A. acknowledges the support from the National Institutes of Health (R01-EB023052; R01HL140618).

DATA AVAILABILITY STATEMENT

The data that support the findings of this study are available from the corresponding author upon reasonable request.

REFERENCES

1. SAXENA AK. Synthetic biodegradable hydrogel (PleuraSeal) sealant for sealing of lung tissue after thoracoscopic resection. Journal of thoracic and cardiovascular surgery (Print) 2010;139(2):496–497.
2. Wain JC, Kaiser LR, Johnstone DW, Yang SC, Wright CD, Friedberg JS, Feins RH, Heitmiller RF, Mathisen DJ, Selwyn MR. Trial of a novel synthetic sealant in preventing air leaks after lung resection. The Annals of Thoracic Surgery 2001;71(5):1623–1629. [PubMed: 11383811]
3. Assmann A, Vegh A, Ghasemi-Rad M, Bagherifard S, Cheng G, Sani ES, Ruiz-Esparza GU, Noshadi I, Lassaletta AD, Gangadharan S and others. A highly adhesive and naturally derived sealant. Biomaterials 2017;140:115–127. [PubMed: 28646685]
4. Li J, Celiz AD, Yang J, Yang Q, Wamala I, Whyte W, Seo BR, Vasilyev NV, Vlassak JJ, Suo Z and others. Tough adhesives for diverse wet surfaces. Science 2017;357(6349):378. [PubMed: 28751604]
5. Annabi N, Shin SR, Tamayol A, Miscuglio M, Bakooshli MA, Assmann A, Mostafalu P, Sun JY, Mithieux S, Cheung L and others. Highly Elastic and Conductive Human-Based Protein Hybrid Hydrogels. Adv Mater 2016;28(1):40–9. [PubMed: 26551969]
6. Blacklow S, Li J, Freedman B, Zeidi M, Chen C, Mooney D. Bioinspired mechanically active adhesive dressings to accelerate wound closure. Science advances 2019;5(7):eaaw3963. [PubMed: 31355332]
7. Li M, Liang Y, He J, Zhang H, Guo B. Two-Pronged Strategy of Biomechanically Active and Biochemically Multifunctional Hydrogel Wound Dressing To Accelerate Wound Closure and Wound Healing. Chemistry of Materials 2020;32(23):9937–9953.

Author Manuscript Author Manuscript Author Manuscript Author Manuscript

8. He J, Shi M, Liang Y, Guo B. Conductive adhesive self-healing nanocomposite hydrogel wound dressing for photothermal therapy of infected full-thickness skin wounds. Chemical Engineering Journal 2020;394:124888.
9. Zhao X, Wu H, Guo B, Dong R, Qiu Y, Ma PX. Antibacterial anti-oxidant electroactive injectable hydrogel as self-healing wound dressing with hemostasis and adhesiveness for cutaneous wound healing. Biomaterials 2017;122:34–47. [PubMed: 28107663]
10. Zhao X, Liang Y, Huang Y, He J, Han Y, Guo B. Physical Double-Network Hydrogel Adhesives with Rapid Shape Adaptability, Fast Self-Healing, Antioxidant and NIR/pH Stimulus-Responsiveness for Multidrug-Resistant Bacterial Infection and Removable Wound Dressing. Advanced Functional Materials 2020;30(17):1910748.
11. Carton CA, Heifetz MD, Kessler LA. Patching of intracranial internal carotid artery in man using a plastic adhesive (Eastman 910 Adhesive). J Neurosurg 1962;19:887–96. [PubMed: 14018979]
12. Carton CA, Kessler LA, Seidenberg B, Hurwitt ES. Experimental studies in the surgery of small blood vessels. IV. Nonsuture anastomosis of arteries and veins, using flanged ring prostheses and plastic adhesive. Surg Forum 1960;11:238–9. [PubMed: 13691166]
13. Annabi N, Tamayol A, Shin SR, Ghaemmaghami AM, Peppas NA, Khademhosseini A. Surgical materials: Current challenges and nano-enabled solutions. Nano today 2014;9(5):574–589. [PubMed: 25530795]
14. Soucy JR, Shirzaei Sani E, Portillo Lara R, Diaz D, Dias F, Weiss AS, Koppes AN, Koppes RA, Annabi N. Photocrosslinkable Gelatin/Tropoelastin Hydrogel Adhesives for Peripheral Nerve Repair. Tissue Eng Part A 2018;24(17–18):1393–1405. [PubMed: 29580168]
15. Carton CA, Heifetz MD, Kessler LA. Patching of intracranial internal carotid artery in man using a plastic adhesive (Eastman 910 adhesive). Journal of neurosurgery 1962;19(10):887–896. [PubMed: 14018979]
16. Carton CA, Kessler LA, Seidenberg B, Hurwitt ES. Experimental studies in surgery of small blood vessels. II. Patching of arteriotomy using a plastic adhesive. J. Neurosurg 1961;18:188–194. [PubMed: 13691165]
17. Soucy JR, Shirzaei Sani E, Portillo Lara R, Diaz D, Dias F, Weiss AS, Koppes AN, Koppes RA, Annabi N. Photocrosslinkable gelatin/tropoelastin hydrogel adhesives for peripheral nerve repair. Tissue Engineering Part A 2018;24(17–18):1393–1405. [PubMed: 29580168]
18. Wolbank S, Pichler V, Ferguson JC, Meinl A, van Griensven M, Goppelt A, Redl H. Non-invasive in vivo tracking of fibrin degradation by fluorescence imaging. Journal of tissue engineering and regenerative medicine 2015;9(8):973–976. [PubMed: 25044309]
19. Montanaro L, Arciola C, Cenni E, Ciapetti G, Savioli F, Filippini F, Barsanti L. Cytotoxicity, blood compatibility and antimicrobial activity of two cyanoacrylate glues for surgical use. Biomaterials 2000;22(1):59–66.
20. Xu C, Lee W, Dai G, Hong Y. Highly Elastic Biodegradable Single-Network Hydrogel for Cell Printing. ACS Appl Mater Interfaces 2018;10(12):9969–9979. [PubMed: 29451384]
21. Yuk H, Varela CE, Nabzdyk CS, Mao X, Padera RF, Roche ET, Zhao X. Dry double-sided tape for adhesion of wet tissues and devices. Nature 2019;575(7781):169–174. [PubMed: 31666696]
22. Zhang YN, Avery RK, Vallmajo-Martin Q, Assmann A, Vegh A, Memic A, Olsen BD, Annabi N, Khademhosseini A. A Highly Elastic and Rapidly Crosslinkable Elastin-Like Polypeptide-Based Hydrogel for Biomedical Applications. Adv Funct Mater 2015;25(30):4814–4826. [PubMed: 26523134]
23. Tavafoghi M, Sheikhi A, Tutar R, Jahangiry J, Baidya A, Haghniaz R, Khademhosseini A. Engineering Tough, Injectable, Naturally Derived, Bioadhesive Composite Hydrogels. Advanced Healthcare Materials;n/a(n/a):1901722.
24. Kloxin AM, Benton JA, Anseth KS. In situ elasticity modulation with dynamic substrates to direct cell phenotype. Biomaterials 2010;31(1):1–8. [PubMed: 19788947]
25. Stowers RS, Allen SC, Suggs LJ. Dynamic phototuning of 3D hydrogel stiffness. Proceedings of the National Academy of Sciences 2015;112(7):1953–1958.
26. Annabi N, Zhang Y-N, Assmann A, Sani ES, Cheng G, Lassaletta AD, Vegh A, Dehghani B, Ruiz-Esparza GU, Wang X and others. Engineering a highly elastic human protein–based sealant for surgical applications. Science Translational Medicine 2017;9(410):eaai7466. [PubMed: 28978753]

Author Manuscript Author Manuscript Author Manuscript Author Manuscript

27. Zhao D, Huang J, Zhong Y, Li K, Zhang L, Cai J. High-strength and high-toughness double-cross-linked cellulose hydrogels: a new strategy using sequential chemical and physical cross-linking. Advanced Functional Materials 2016;26(34):6279–6287.
28. Berry M, Engler A, Woo Y, Pirolli T, Bish L, Jayasankar V, Morine K, Gardner T, Discher D, Sweeney H. Mesenchymal stem cell injection after myocardial infarction improves myocardial compliance. American journal of physiology. Heart and circulatory physiology 2006;290:H2196–203. [PubMed: 16473959]
29. Diekman BO, Christoforou N, Willard VP, Sun H, Sanchez-Adams J, Leong KW, Guilak F. Cartilage tissue engineering using differentiated and purified induced pluripotent stem cells. Proceedings of the National Academy of Sciences 2012;109(47):19172–19177.
30. Annabi N, Shin SR, Tamayol A, Miscuglio M, Bakooshli MA, Assmann A, Mostafalu P, Sun J-Y, Mithieux S, Cheung L and others. Highly Elastic and Conductive Human-Based Protein Hybrid Hydrogels. Advanced Materials 2016;28(1):40–49. [PubMed: 26551969]
31. Han L, Yan L, Wang K, Fang L, Zhang H, Tang Y, Ding Y, Weng L-T, Xu J, Weng J and others. Tough, self-healable and tissue-adhesive hydrogel with tunable multifunctionality. NPG Asia Materials 2017;9(4):e372–e372.
32. Sun J-Y, Zhao X, Illeperuma WR, Chaudhuri O, Oh KH, Mooney DJ, Vlassak JJ, Suo Z. Highly stretchable and tough hydrogels. Nature 2012;489(7414):133–136. [PubMed: 22955625]
33. Lang N, Pereira MJ, Lee Y, Friehs I, Vasilyev NV, Feins EN, Ablasser K, O'Cearbhaill ED, Xu C, Fabozzo A. A blood-resistant surgical glue for minimally invasive repair of vessels and heart defects. Science translational medicine 2014;6(218):218ra6–218ra6.
34. Li J, Celiz A, Yang J, Yang Q, Wamala I, Whyte W, Seo B, Vasilyev N, Vlassak J, Suo Z. Tough adhesives for diverse wet surfaces. Science 2017;357(6349):378–381. [PubMed: 28751604]
35. Liao IC, Moutos FT, Estes BT, Zhao X, Guilak F. Composite three-dimensional woven scaffolds with interpenetrating network hydrogels to create functional synthetic articular cartilage. Advanced functional materials 2013;23(47):5833–5839. [PubMed: 24578679]
36. Yang J, Han C-r, Xu F, Sun R-c. Simple approach to reinforce hydrogels with cellulose nanocrystals. Nanoscale 2014;6(11):5934–5943. [PubMed: 24763379]
37. Annabi N, Shin SR, Tamayol A, Miscuglio M, Bakooshli MA, Assmann A, Mostafalu P, Sun JY, Mithieux S, Cheung L. Highly elastic and conductive human-based protein hybrid hydrogels. Advanced materials 2016;28(1):40–49. [PubMed: 26551969]
38. Guo Q, Chen J, Wang J, Zeng H, Yu J. Recent progress in synthesis and application of mussel-inspired adhesives. Nanoscale 2020;12(3):1307–1324. [PubMed: 31907498]
39. Cohen B, Pinkas O, Foox M, Zilberman M. Gelatin–alginate novel tissue adhesives and their formulation–strength effects. Acta biomaterialia 2013;9(11):9004–9011. [PubMed: 23851174]
40. Ahn BK, Das S, Linstadt R, Kaufman Y, Martinez-Rodriguez NR, Mirshafian R, Kesselman E, Talmon Y, Lipshutz BH, Israelachvili JN. High-performance mussel-inspired adhesives of reduced complexity. Nature communications 2015;6(1):1–7.
41. Maier GP, Rapp MV, Waite JH, Israelachvili JN, Butler A. Adaptive synergy between catechol and lysine promotes wet adhesion by surface salt displacement. Science 2015;349(6248):628–632. [PubMed: 26250681]
42. Wang R, Li J, Chen W, Xu T, Yun S, Xu Z, Xu Z, Sato T, Chi B, Xu H. A biomimetic mussel-inspired ε-poly-l-lysine hydrogel with robust tissue-anchor and anti-infection capacity. Advanced Functional Materials 2017;27(8):1604894.
43. Meredith HJ, Jenkins CL, Wilker JJ. Enhancing the adhesion of a biomimetic polymer yields performance rivaling commercial glues. Advanced functional materials 2014;24(21):3259–3267.
44. Zhang L, Liu M, Zhang Y, Pei R. Recent Progress of Highly Adhesive Hydrogels as Wound Dressings. Biomacromolecules 2020;21(10):3966–3983. [PubMed: 32960043]
45. Yue K, Trujillo-de Santiago G, Alvarez MM, Tamayol A, Annabi N, Khademhosseini A. Synthesis, properties, and biomedical applications of gelatin methacryloyl (GelMA) hydrogels. Biomaterials 2015;73:254–71. [PubMed: 26414409]
46. Kaneko N, Ghovvati M, Komuro Y, Guo L, Khatibi K, Ponce Mejia LL, Saber H, Annabi N, Tateshima S. A new aspiration device equipped with a hydro-separator for acute ischemic stroke due to challenging soft and stiff clots. Interv Neuroradiol 2021:15910199211015060.

Author Manuscript Author Manuscript Author Manuscript Author Manuscript

47. Montazerian H, Baidya A, Haghniaz R, Davoodi E, Ahadian S, Annabi N, Khademhosseini A, Weiss PS. Stretchable and Bioadhesive Gelatin Methacryloyl-Based Hydrogels Enabled by in Situ Dopamine Polymerization. ACS Applied Materials & Interfaces 2021;13(34):40290–40301. [PubMed: 34410697]

48. Liu Y, Meng H, Konst S, Sarmiento R, Rajachar R, Lee BP. Injectable dopamine-modified poly(ethylene glycol) nanocomposite hydrogel with enhanced adhesive property and bioactivity. ACS Appl Mater Interfaces 2014;6(19):16982–92. [PubMed: 25222290]

49. Wang Y, Cao X, Ma M, Lu W, Zhang B, Guo Y. A GelMA-PEGDA-nHA Composite Hydrogel for Bone Tissue Engineering. Materials (Basel) 2020;13(17).

50. Annabi N, Rana D, Shirzaei Sani E, Portillo-Lara R, Gifford JL, Fares MM, Mithieux SM, Weiss AS. Engineering a sprayable and elastic hydrogel adhesive with antimicrobial properties for wound healing. Biomaterials 2017;139:229–243. [PubMed: 28579065]

51. Zhang W, Wang R, Sun Z, Zhu X, Zhao Q, Zhang T, Cholewinski A, Yang F, Zhao B, Pinnaratip R and others. Catechol-functionalized hydrogels: biomimetic design, adhesion mechanism, and biomedical applications. Chemical Society Reviews 2020;49(2):433–464. [PubMed: 31939475]

52. Yavvari PS, Pal S, Kumar S, Kar A, Awasthi AK, Naaz A, Srivastava A, Bajaj A. Injectable, Self-Healing Chimeric Catechol-Fe(III) Hydrogel for Localized Combination Cancer Therapy. ACS Biomaterials Science & Engineering 2017;3(12):3404–3413. [PubMed: 33445379]

53. Rahimnejad M, Zhong W. Mussel-inspired hydrogel tissue adhesives for wound closure. RSC Advances 2017;7(75):47380–47396.

54. Huang W-C, Ali F, Zhao J, Rhee K, Mou C, Bettinger CJ. Ultrasound-Mediated Self-Healing Hydrogels Based on Tunable Metal–Organic Bonding. Biomacromolecules 2017;18(4):1162–1171. [PubMed: 28245355]

55. Gong C, Lu C, Li B, Shan M, Wu G. Injectable dopamine-modified poly(α,β-aspartic acid) nanocomposite hydrogel as bioadhesive drug delivery system. Journal of Biomedical Materials Research Part A 2017;105(4):1000–1008. [PubMed: 27739644]

56. Kazemzadeh-Narbat M, Annabi N, Khademhosseini A. Surgical sealants and high strength adhesives. Materials Today 2015;18(4):176–177.

Author Manuscript Author Manuscript Author Manuscript Author Manuscript

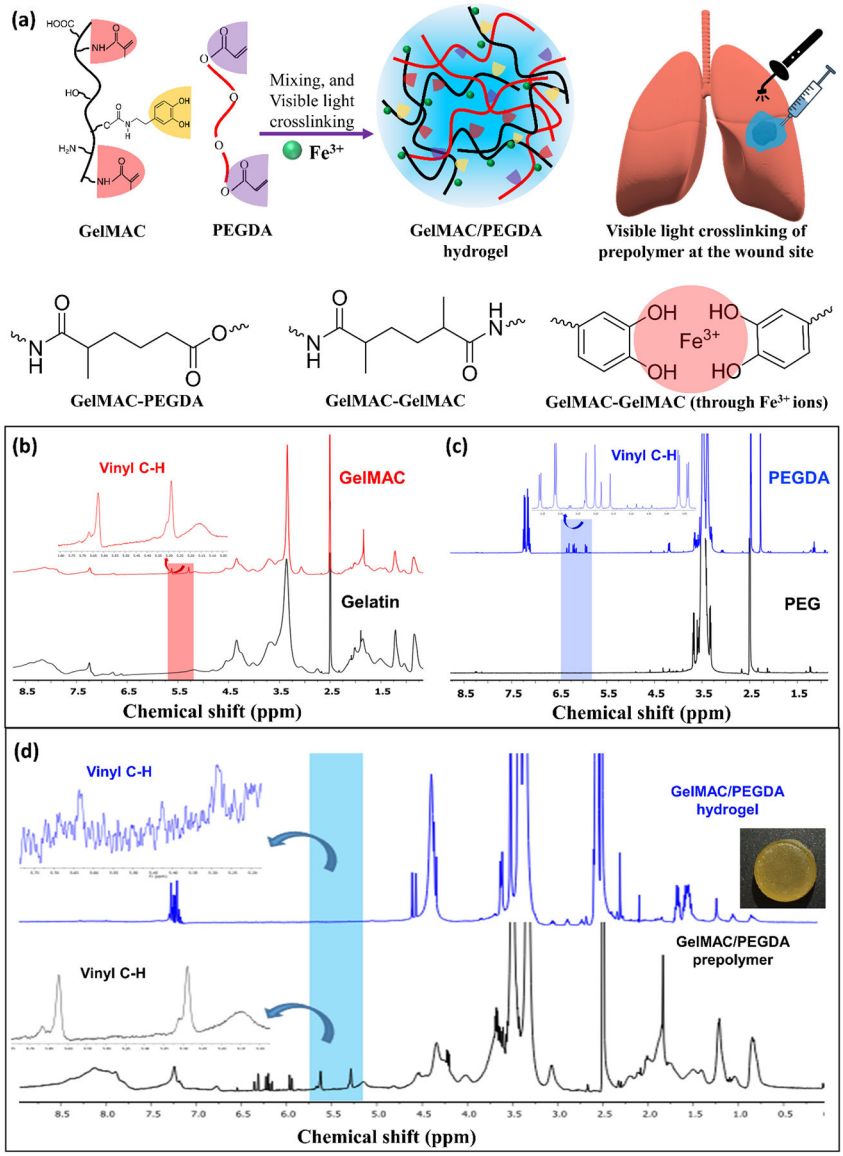

FIGURE 1.

Synthesis and characterization of GelMAC/PEGDA hydrogels. (a) Schematic representation for the fabrication of GelMAC/PEGDA hydrogels by visible light crosslinking of prepolymer solutions, and interactions between GelMAC and PEGDA comprised of covalent bonding upon photocrosslinking and ferric ion induced non-covalent chelation interactions. (b) ^{1}H NMR spectrum of porcine gelatin and GelMAC. (c) ^{1}H NMR spectrum of PEG and PEGDA. (d) ^{1}H NMR spectrum of GelMAC/PEGDA prepolymer and GelMAC/PEGDA crosslinked.

Author Manuscript Author Manuscript Author Manuscript Author Manuscript

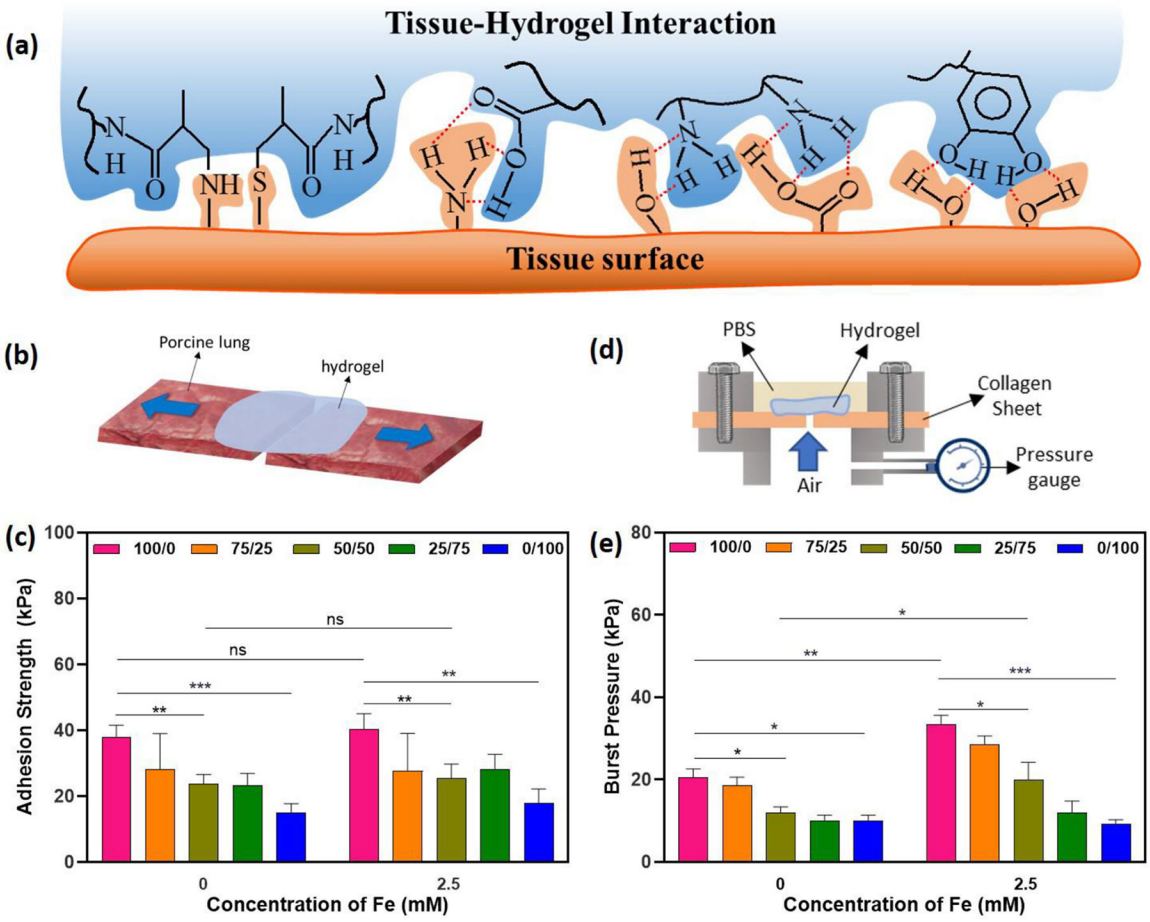

FIGURE 2.

In vitro adhesive properties of the GelMAC/PEGDA hydrogels. (a) Schematic representation of tissue-hydrogel interaction. (b) Schematic representation of wound closure test (c) Adhesion strength for GelMAC/PEGDA hydrogels containing varying ratios of GelMAC and PEGDA. (d) Schematic representation of burst pressure test. (e) Burst pressure of elastic hydrogels fabricated with varying ratios of GelMAC and PEGDA. Hydrogels were prepared at 20% (w/v) total polymer concentration and 4 min visible light exposure time. Error bars indicate standard error of the means, asterisks mark significance levels of $p < 0.05$ (*), $p < 0.01$ (**), $p < 0.001$ (***), and $p < 0.0001$ (****).

Author Manuscript Author Manuscript Author Manuscript Author Manuscript

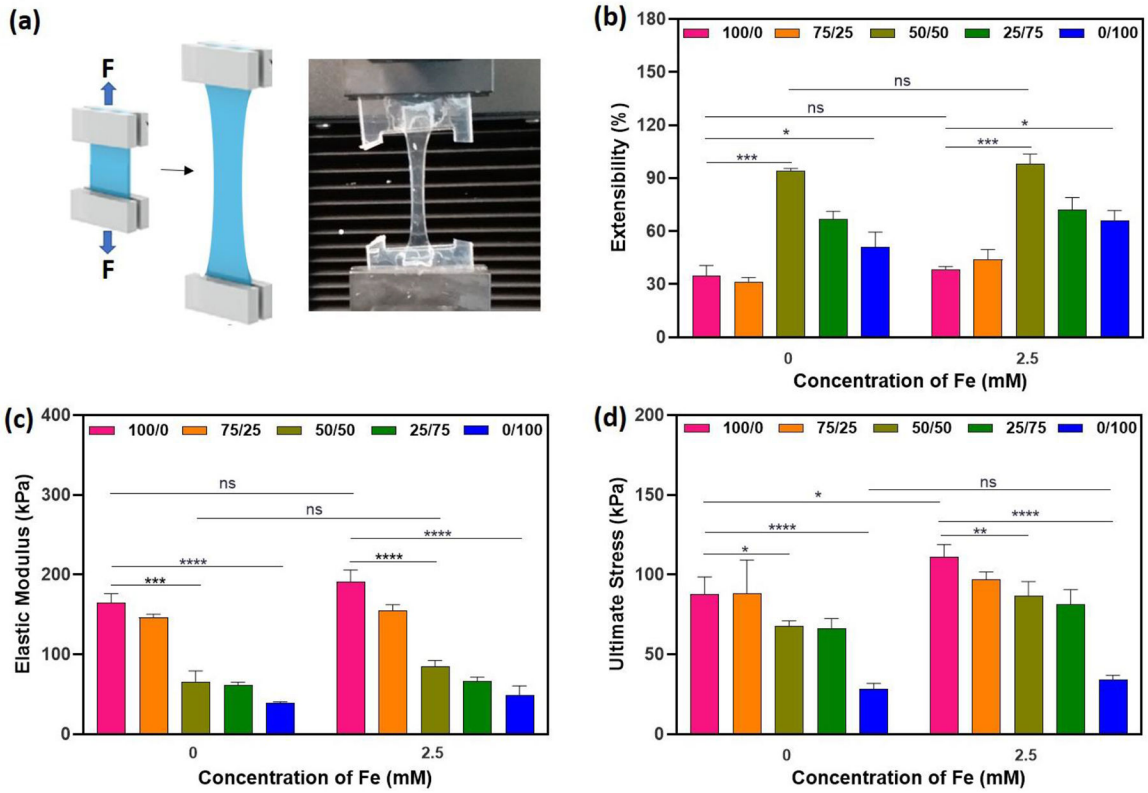

FIGURE 3.

Tensile properties of GelMAC/PEGDA hydrogels. (a) Schematic and representative image of tensile test. (b) Extensibility, (c) Elastic modulus, and (d) Ultimate stress of the fabricated hydrogels containing varying ratios of GelMAC and PEGDA. Hydrogels were prepared at 20% (w/v) total polymer concentration and 4 min visible light exposure time. Error bars indicate standard error of the means, asterisks mark significance levels of $p < 0.05$ (*), $p < 0.01$ (**), $p < 0.001$ (***), and $p < 0.0001$ (****).

Author Manuscript Author Manuscript Author Manuscript Author Manuscript

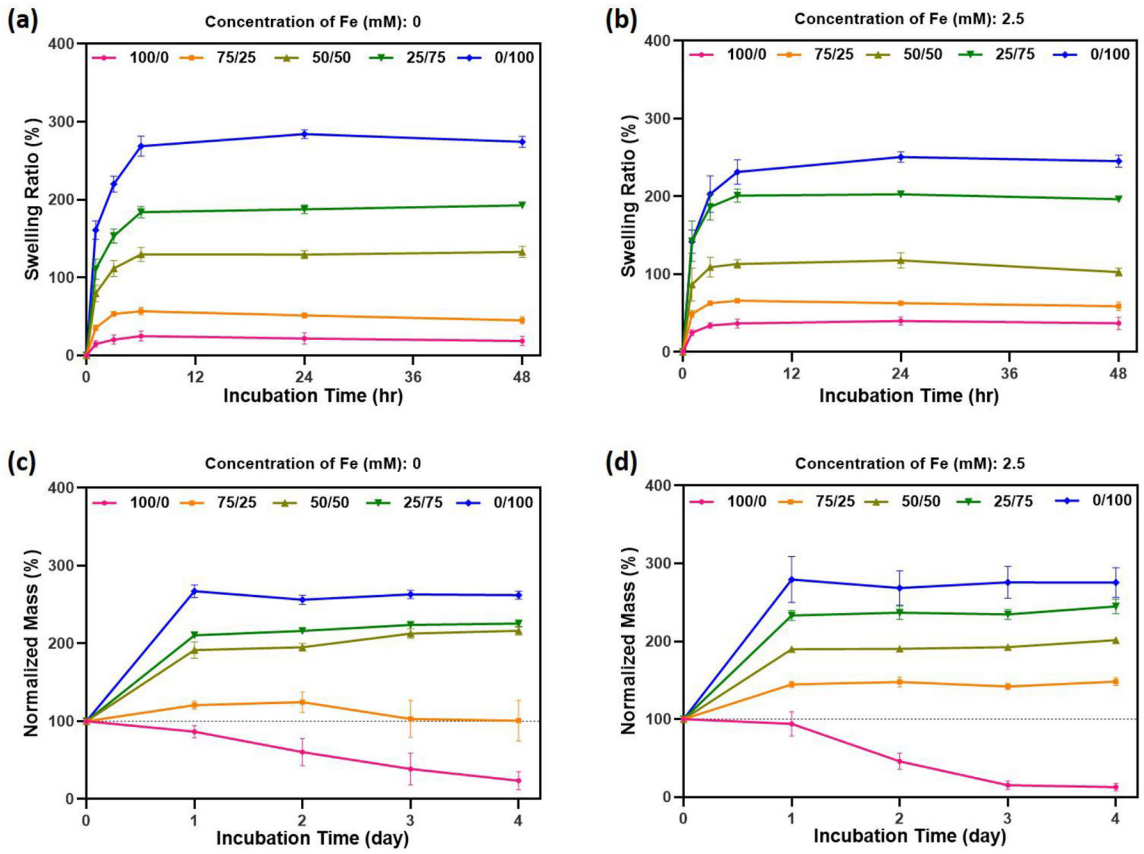

FIGURE 4.

In vitro swelling behavior and normalized mass of GelMAC/PEGDA hydrogels. *In vitro* swelling behavior of the fabricated hydrogels containing varying ratios of GelMAC and PEGDA incubated in DPBS at 37°C (a) without ferric ions, (b) with 2.5 mM ferric ions. Normalized mass of the GelMAC/PEGDA hydrogels containing varying ratios of GelMAC and PEGDA incubated in 5 U/mL of collagenase type II in DPBS at 37°C (c) without ferric ions, (d) with 2.5 mM ferric ions solution. Hydrogels were prepared at 20% (w/v) total polymer concentration and 4 min visible light exposure time. Error bars indicate standard error of the means.

Author Manuscript Author Manuscript Author Manuscript Author Manuscript

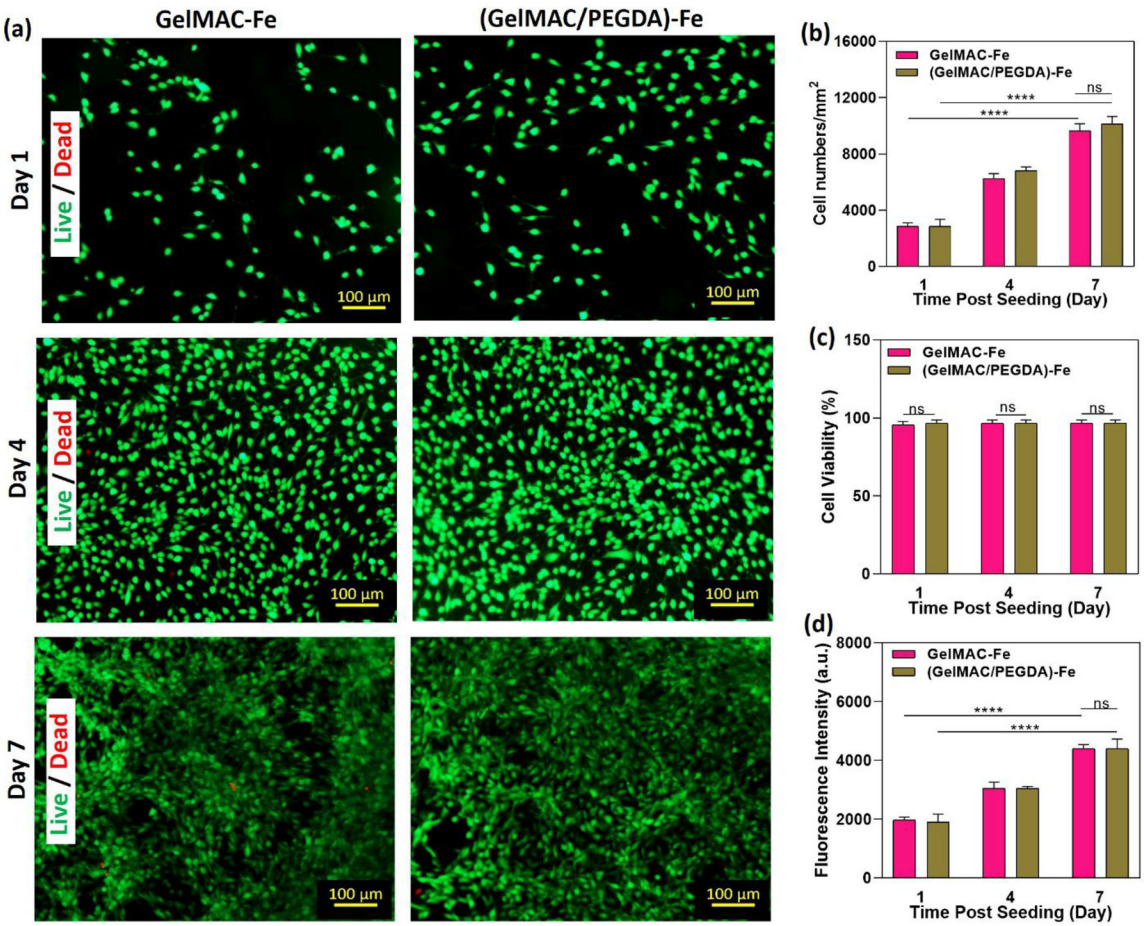

FIGURE 5.

In vitro 2D seeding of NIH 3T3 fibroblast cells on the GelMAC-Fe and (GelMAC/PEGDA)-Fe hydrogels. (a) Representative live/dead images of the cells seeded on the surface of fabricated hydrogels after 1, 4, and 7 days post-seeding. (b) Quantification of cell proliferation based on live/dead assay at days 1, 4, and 7 post-seeding. (c) Quantification of the viability of 3T3 cells seeded on the hydrogels using live/dead assays on days 1, 4, and 7 post-culture. (d) Quantification of metabolic activity of 3T3 cells seeded on the hydrogels using PrestoBlue assay on days 1, 4, and 7 post-culture. Hydrogels were applied at 20% (w/v) total polymer concentration and 20 s visible light exposure time. Error bars indicate standard error of the means, asterisks mark significance levels of **** $p < 0.0001$).

Author Manuscript Author Manuscript Author Manuscript Author Manuscript

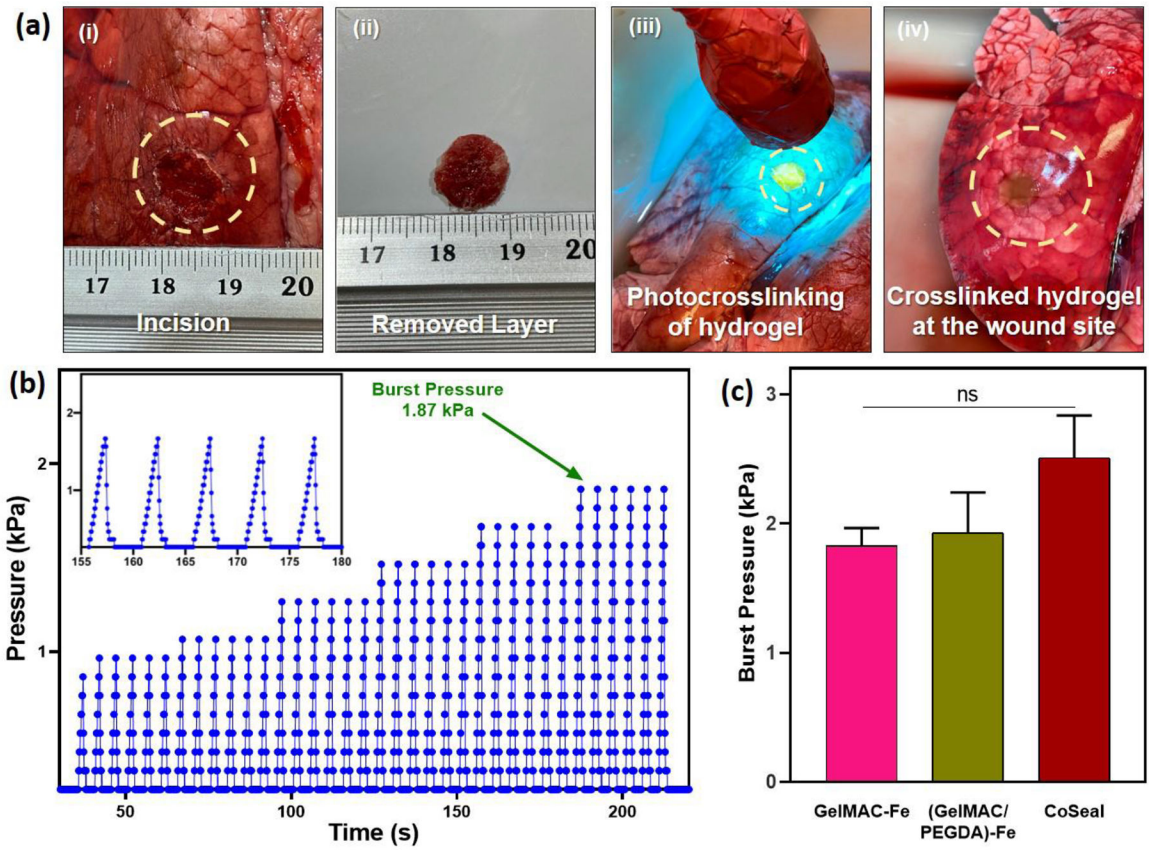

FIGURE 6.

Ex vivo test to evaluate the sealing capability of the (GelMAC/PEGDA)-Fe sealant using a porcine lung incision model. (a) Creating incision, injecting hydrogel and photocrosslinking in situ: (a-i) incision created, (a-ii) removed visceral pleural layer, (a-iii) photocrosslinking of hydrogel, (a-iv) crosslinked hydrogel at the wound site. (b) A representative graph depicting the stepwise pressure increasing over time during testing (c) Burst pressure of GeMAC-Fe, (GelMAC/PEGDA)-Fe, and CoSeal. Hydrogels were formed at 20% (w/v) total polymer concentration and 4 min visible light exposure time.